

On-board Federated Learning for Satellite Clusters with Inter-Satellite Links

Nasrin Razmi, *Student Member, IEEE*, Bho Matthiesen, *Member, IEEE*,
 Armin Dekorsy, *Senior Member, IEEE*, and Petar Popovski, *Fellow, IEEE*

Abstract

The emergence of mega-constellations of interconnected satellites has a major impact on the integration of cellular wireless and non-terrestrial networks (NTN). This paper studies the problem of running a federated learning (FL) algorithm within a low Earth orbit (LEO) constellation of satellites connected with intra-orbit inter-satellite links (ISL). Satellites apply on-board machine learning and transmit the local parameters to the parameter server (PS). The main contribution is a novel approach to enhance FL in satellite constellations using intra-orbit ISLs. The key idea is to rely on the predictability of satellite visits to create a system design in which ISLs mitigate the impact of intermittent connectivity and transmit the aggregated parameters to the PS. We first devise a synchronous FL, which is then extended towards an asynchronous FL for the case of sparse satellite visits to the PS. An efficient use of the satellite resources is attained by sparsification-based compression the aggregated parameters of each orbit before forwarding to the PS. Performance is evaluated in terms of accuracy and the required size of data to be transmitted. The numerical results indicate a faster convergence rate of the presented approach compared with the state-of-the-art FL on satellite constellations.

Index Terms

Low Earth orbit, mega-constellations, intra-orbit inter-satellite links, federated learning, sparsification.

N. Razmi, B. Matthiesen, and A. Dekorsy are with the Gauss-Olbers Center, c/o University of Bremen, and the Department of Communications Engineering, University of Bremen, 28359 Bremen, Germany (e-mail: {razmi,matthiesen,dekorsy}@ant.uni-bremen.de). P. Popovski is with the Department of Electronic Systems, Aalborg University, 9100 Aalborg, Denmark (e-mail: petarp@es.aau.dk). P. Popovski is also holder of the U Bremen Excellence Chair in the Department of Communications Engineering, University of Bremen, 28359 Bremen, Germany.

This work is supported in part by the German Research Foundation (DFG) under Germany's Excellence Strategy (EXC 2077 at University of Bremen, University Allowance).

Part of this work was presented at the IEEE International Conference on Communications (ICC 2022), Seoul, South Korea, May, 2022 [1].

I. INTRODUCTION

Satellite constellations have been an essential component of modern communication and remote sensing systems for decades. Recent advances in satellite technology and the emergence of interconnected mega constellations in low earth orbit (LEO), are revolutionizing the way we collect and process data from space [2]–[4]. Unlike the previous cellular generations that were exclusively focused on terrestrial networks, mega-constellations and Non-Terrestrial Networks (NTN) are seen as the integral part of 5G and the upcoming 6G wireless systems [5]. Consisting of thousands of satellites, these constellations have the potential to process vast amounts of data. Conventional central processing of this collected data involves significant challenges, including communication delays, limited bandwidth and storage, as well as data ownership concerns [6], [7]. The on-board intelligence of satellites increases steadily [4], [8], [9], pushing towards in-orbit data preservation and learning to conserve bandwidth and energy, avoid overloading of ground-satellite links (GSLs), and enable native artificial intelligence in space.

Satellite federated learning (SFL) has emerged as a promising solution to address these challenges [7], [10], as an instance of distributed machine learning (ML) that enables satellites to collaboratively learn a model without exchanging raw data. With federated learning (FL), each satellite trains a local model with its own data and sends only the updated model parameters to be aggregated at a central *parameter server (PS)*. FL has the potential to reduce both communication cost and training delay. The first step towards SFL was made in [10], where each satellite acts as an individual collaborator towards the PS, located within a terrestrial ground station (GS). As [10] does not assume existence of inter-satellite links (ISLs), the synchronization of intermediate results with the PS requires direct link from each satellite to the GS. Each LEOs satellite has only a very short communication window per orbital period towards the terrestrial PS. This, as well as the fact the link between a fixed GS and a satellite vanishes behind the horizon for several hours after a few orbital periods, leads to a connectivity bottleneck that severely inhibits convergence speed of a plain FL. Thus, instead of using conventional synchronous FL, [10] advantageously uses the sporadic, but predictable, satellite connectivity to roll out an asynchronous aggregation.

Newer satellites, especially within the context of mega constellations [11]–[13], rely increasingly on ISLs and multi-hop routing. In this paper, we consider a SFL setup with ISLs, focusing on links between adjacent satellites within the same orbital plane, as in that case the satellites have stable relative positions and thereby stable links. However, a direct implementation of multi-hop

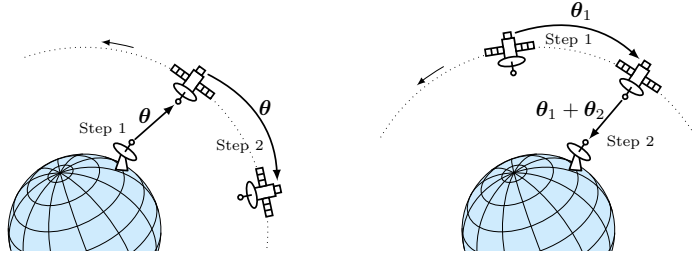


Fig. 1. Global model distribution (left) and collection of local updates (right) using intra-orbit inter-satellite communication.

routing leads to network traffic growing quadratically in the number of satellites and a high load on links towards the PS, as each client update will be treated as a common unicast message. Leveraging the structure of FL traffic along with in-network aggregation [14], communication can be limited to a single outgoing message per satellite and a global iteration during the aggregation phase. Moreover, most of these transmissions use intra-orbit ISLs instead of the more challenging PS link, resulting energy saving and reduced communication load at the PS.

Fig. 1 illustrates the key idea through an example of connectivity bottleneck in SFL using two satellites at 550 km altitude, spaced 45° apart within the same orbital plane. The PS is located in a GS and both satellites are participating in a FL procedure with their local data sets. A single pass over the GS, i.e., the time the satellite and the GS can communicate, is less than 10 minutes, while a single orbital period is 95 minutes. Assume that the computation of this update takes 15 minutes. Let one of the satellites be selected by the PS to compute an update to the global model. The satellite will collect the current global model on the first pass and return the result on the next pass. This incurs a delay of roughly one orbital period, which is more than one hour in excess of the computation time. If both satellites are supposed to compute an update then, upon the first pass, each satellite will collect the current model version and start computing. The first satellite will pass the PS for the second time and deliver the update. However, in a synchronous FL procedure, the PS will not update the global model until all updates are received. Hence, the first satellite will not have a new model version available to iterate upon during the offline period following the second pass. Differently from this, when ISLs are available, the first satellite can transmit this global model to the second satellite directly after receiving it. Then, both satellites compute the update in parallel and the second satellite can collect and deliver both updates to the GS during its first pass. This is illustrated in Fig. 1. The time for a single global iteration is reduced from over one orbital period to less than 20 minutes by this approach, while the traffic

at the PS is reduced by 50 %. Implementing this idea requires careful system design and route planning, relying upon the inherent determinism of satellite movement.

The objective of this paper is to present a system design for SFL within a LEO satellite mega-constellation in which the satellites within the same orbital plane are connected via ISLs to the adjacent nodes, forming a ring network. Each satellite has the capability to communicate with an out-of-orbit entity, such as GS, that orchestrates the training process. The external orchestration is needed as the satellites are not necessarily able to communicate across orbital planes; at the same time it creates a connectivity bottleneck. The contributions of this paper are:

- Design of a distributed system for SFL, supporting client clustering, synchronous and asynchronous orchestration, and consistent decentralized routing decisions.
- Development of a communication scheme for SFL that takes advantage of intra-orbit ISLs. Due to the co-design of predictive routing and in-network aggregation, the convergence time is reduced markedly, while not increasing the communication load.
- Extension of the proposed communication scheme to accommodate gradient sparsification and in-network aggregation for bandwidth-efficiency. This includes the development of a novel estimator for the number of non-zero elements in the sum of sparse vectors.
- An effective method to prevent biased solutions for asynchronous aggregation in satellite constellations connected with ISLs. This is necessary after improving connectivity with ISLs, as simple opportunistic scheduling can result in a small subset of clusters dominating the training process for several hours.
- We have evaluated the performance of the proposed system in several setups. The numerical results highlight a major increase in convergence speed (~ 7 times) due to the use of ISLs and ~ 10 times reduction of communication load based on our in-network aggregation approach.

We remark that the proposed system is agnostic to the actual federated optimization (FO) procedure, as long as it supports partial aggregation as discussed in Section IV-A. Hence, the system performance can be further improved using conventional fine-tuning of FO algorithms and ML model-specific hyperparameters [15]. Finally, we note that the primary performance metric in this paper is the convergence time measured by a (simulated) wall clock. Conventional metrics for FL algorithms are model test accuracy versus the number of global iterations or the number of gradient computations. This is sensible as the focus in these studies is on improved computational efficiency. Instead, the key challenge that sets SFL apart from conventional scenarios is the

connectivity bottleneck implied by the laws of orbital mechanics, potentially leading to extensive delays between iterations. Success in overcoming these obstacles is best measured in the number of global iterations the distributed system can manage within a certain period. As with any communication system, another important metric is bandwidth-efficiency, especially in GSLs.

A. Related Work

A detailed technical model of SFL was introduced [10], while [6] considered it in a more general context of satellite-based computing networks. A broad overview of the different scenarios encountered in SFL, together with a discussion of the technical challenges for each scenario, is presented in [7]. The technical details of several of the ideas sketched in [7] are provided in this paper. Aerial FL [16] is a setup that is complementary to SFL, in which the PS is operated within a satellite to orchestrate a planet-side FL process. Closely related to that are the satellite-assisted internet of remote things system architectures considered in [17] and [18].

A broad classification of current work on SFL can be made based on the presence and usage of ISLs. The model in [10] considers the case without ISLs, identifies the connectivity bottleneck, and proposes a satellite-specific asynchronous FL algorithm as solution. This work is extended in [19] with a scheduling algorithm that exploits the inherent determinism of satellite trajectories. Another scheduling approach based on buffered asynchronous FL is proposed in [20], aiming to balance local model staleness and idle times. Lacking a thorough benchmark against the state-of-the-art, the gain of the complicated scheduling algorithm in [20] remains an open question. Staleness in asynchronous SFL is further investigated in [21], which introduces an asynchronous update rule based on the notion that staleness effects in SFL are similar in consecutive training epochs. In [22] the connection bottleneck is tackled by combining synchronous orchestration with a dynamic aggregation rule that ignores stragglers. However, the primary reason for the feasibility of synchronous terrestrial orchestration is the usage of multiple geographically distributed GSs that act as a distributed PS. While the authors observe correctly that latency between GSs is small compared to GSLs, mechanisms to either ensure consistency between GSs or a hierarchical FL approach would be required in a practical system implementation of [22].

An alternative means to improving connectivity is the usage of ISLs instead of a distributed PS, as proposed in the conference version of this paper [1]. The communication strategy from [1] is adopted in [23] and combined with a distributed PS implemented within interconnected high-altitude platform stations (HAPSs). This is extended in [24] to asynchronous aggregation

with multiple HAPSs. A modified version of [1] is proposed in [25], consisting of a decentralized implementation of predictive routing, which might lead to inconsistent routing decisions, and the absence of incremental aggregation (see Section IV-A), which leads to a quadratic traffic growth within each orbital plane. FL in a completely connected satellite constellation is considered in [26], in which training participation is required only from the satellites that are within a cluster that is close to the GS. A decentralized learning system, without PS, leveraging inter- and intra-orbit ISLs is proposed in [27]. Decentralized learning in LEO satellite constellations under very realistic satellite system assumptions is considered in [28] for a semi-supervised classification task. Finally, [29] treats FL-aware routing and resource allocation for SFL.

B. Notation

Scalars are represented in a normal font x , while vectors in bold \mathbf{x} . The Euclidean norm of a vector \mathbf{x} is $\|\mathbf{x}\|$. The angle between two vectors \mathbf{x}_1 and \mathbf{x}_2 is $\angle(\mathbf{x}_1, \mathbf{x}_2)$. Sets are denoted by \mathcal{X} , and the cardinality of \mathcal{X} is $|\mathcal{X}|$. Removing an element x_i from the set \mathcal{X} is denoted by $\mathcal{X} \setminus \{x_i\}$. In a graph $\mathcal{G} = (\mathcal{V}, \mathcal{E})$ with vertices \mathcal{V} and edges \mathcal{E} , the neighborhood of any vertex $v \in \mathcal{V}$ is denoted as $\mathcal{N}(v)$. If \mathcal{G} is directed, $\mathcal{N}^-(v)$ and $\mathcal{N}^+(v)$ denote the incoming and outgoing neighborhood of v , respectively. The operators $\Pr(\cdot)$, \mathbb{E} , and $I(\cdot)$ are the probability, expected value, and indicator function, respectively. Integer rounding is denoted by $\lfloor \cdot \rfloor$ and $\lceil \cdot \rceil$.

II. SYSTEM MODEL

The constellation has P orbital planes, where each orbit p contains K_p satellites \mathcal{K}_p such that $\mathcal{K}_{p_1} \cap \mathcal{K}_{p_2} = \emptyset$, for all $p_1 \neq p_2$. The set of all satellites within the constellation is denoted as $\mathcal{K} = \bigcup_{p=1}^P \mathcal{K}_p = \{k_{1,1}, \dots, k_{P,K_p}\}$ with the total number of satellites $K = \sum_{p=1}^P K_p$. Each satellite k follows a trajectory $\mathbf{s}_k(t)$ around Earth with orbital period $T_p = 2\pi\sqrt{\frac{a_k^3}{\mu}}$, i.e., $\mathbf{s}_k(t) \approx \mathbf{s}_k(t+nT_p)$ for all integer n , where a_k is the semi-major axis of satellite k and $\mu = 3.98 \times 10^{14} \text{ m}^3/\text{s}^2$ is the geocentric gravitational constant. For circular orbits, the semi-major axis is $a_k = r_E + h_k$ with h_k being the satellite's altitude above the Earth's surface and $r_E = 6371 \text{ km}$ the Earth radius. The satellites within an orbital plane p follow the same trajectory and are assigned unique IDs $\mathcal{K}_p = \{k_{p,1}, \dots, k_{p,K_p}\}$ such that satellite $k_{p,i+1}$ is behind $k_{p,i}$. If the satellites are distributed

equidistantly within the orbital plane, we have $\mathbf{s}_{k_p,1}(t) \approx \mathbf{s}_{k_p,2}(t - T_p/K_p) \approx \mathbf{s}_{k_p,3}(t - 2T_p/K_p) \approx \dots$.¹ Coordinates are in an Earth-centric reference frame.

A. Communication Model

Each satellite has three communication devices, two of which are for intra-orbit communications. The third one is for communication outside of its orbital plane, either a ground-to-satellite link or an ISL towards a satellite in another orbit. Communication with an Earth-based GS is feasible if the satellite is visible from the GS at an elevation angle $\frac{\pi}{2} - \angle(\mathbf{s}_{GS}, \mathbf{s}_k(t) - \mathbf{s}_{GS}) \geq \alpha_e$, where α_e is the minimum elevation angle [3], [30] and \mathbf{s}_{GS} is the position of the GS. While this condition is satisfied, we assume communication is possible at a fixed rate. For ISLs, communication is feasible if the line of sight is not obstructed by the Earth. With lower atmospheric layers degrading the link quality, a sensible assumption is to consider an ISLs to be feasible if it does not enter the atmosphere below the Thermosphere [31], starting at approximately 80 km above sea level. This translates to a maximum slant range $d_{Th}(t; k_1, k_2) = \sqrt{\|\mathbf{s}_{k_1}(t)\|^2 - r_T^2} + \sqrt{\|\mathbf{s}_{k_2}(t)\|^2 - r_T^2}$ for any two satellites k_1, k_2 , where $r_T = r_E + 80$ km. For circular orbits, this threshold is the constant $d_{Th}(k_1, k_2) = \sqrt{(h_{k_1} + r_E)^2 - r_T^2} + \sqrt{(h_{k_2} + r_E)^2 - r_T^2}$. We assume communication at a fixed rate is possible between satellites k_1 and k_2 if their distance at time t is $d(t; k_1, k_2) \leq d_{Th}(t; k_1, k_2)$.

The most stable link usage is to connect each satellite to its two closest orbital neighbors, effectively forming a ring network [32]. The two neighbors of satellite $k_{p,i}$ are $\mathcal{N}(k_{p,i}) = \{k_{p,i-1}, k_{p,i+1}\}$. Here, the satellite indices $i - 1$ and $i + 1$ are modulo K_p , which is a convention we will adopt throughout this paper until further notice. Following the previous discussion, the data rate between any two satellites $k_1, k_2 \in \mathcal{K}$ within the constellation is fixed to $r(t; k_1, k_2) = \rho_{k_1, k_2}$ if $k_2 \in \mathcal{N}(k_1)$ and communication is feasible, and zero otherwise. For the out-of-orbit communication link, we assume there is a single communication partner of interest, denoted as the PS. Then, the rate function of satellite k 's, $k \in \mathcal{K}$, link towards the PS is similarly defined as $r_{PS}(t; k) = \rho_{k, PS}$ if communication is feasible and zero otherwise.

B. Computation Model

The satellites within the constellation collaboratively train a ML model from data \mathcal{D} collected at the satellites. The ML model is known at all satellites and fully defined by its model parameter

¹Under the assumption of perfect Keplerian orbits, we can replace ' \approx ' with '=' in all statements on trajectories. With real-world orbits being subject to orbital perturbations and station keeping maneuvers, these relations do not hold exactly and we only state them here to introduce notation and some general concepts on an abstraction level suitable for this paper.

vector $\mathbf{w} \in \mathbb{R}^{n_d}$. The goal is to find a solution to the optimization problem

$$\min_{\mathbf{w}} F(\mathbf{w}), \quad (1)$$

where the global loss function $F(\mathbf{w}) = \frac{1}{D} \sum_{\mathbf{x} \in \mathcal{D}} f(\mathbf{x}; \mathbf{w})$, with $D = |\mathcal{D}|$, measures the performance of the ML model with respect to the data set \mathcal{D} for a certain set of model parameters \mathbf{w} and a potentially nonconvex per-sample loss function $f(\mathbf{x}; \mathbf{w})$.

Regarding (1), we make two fundamental assumptions: (i) the computational resources at the satellites are limited such that a distributed solution of (1) is necessary; (ii) the data set \mathcal{D} is distributed across the constellation and communicating this data is not feasible; i.e., each satellite has a local data set \mathcal{D}_k such that $\mathcal{D} = \bigcup_{k \in \mathcal{K}} \mathcal{D}_k$, which is not shared with any other participants in the training process. Due to the local data sets assumption and the limited connectivity, this distributed ML scenario is an instance of a FL [33]. However, in contrast to a conventional FL setup, here client participation is under central control, the connectivity is mostly deterministic and predictable, and the number of devices is orders of magnitude lower.

In FL, (1) is solved iteratively using a modified distributed stochastic gradient descent (DSGD) procedure.² This algorithm is motivated by the linearity of the gradient and the observation that the objective function is separable as $F(\mathbf{w}) = \frac{1}{D} \sum_{k \in \mathcal{K}} D_k F_k(\mathbf{w})$ with $F_k(\mathbf{w}) = \frac{1}{D_k} \sum_{\mathbf{x} \in \mathcal{D}_k} f(\mathbf{x}; \mathbf{w})$ and $D_k = |\mathcal{D}_k|$. The optimization process is orchestrated by a central PS, which maintains the current iteration of the global model parameters \mathbf{w} , distributes these to the clients for further refinement, and collects the results. In contrast to conventional FL, we assume that every client participates in every iteration of the solution process due to the relatively small number of clients. Since satellites within the constellation are only connected to their orbital neighbors, communication across orbital planes is only feasible via the out-of-constellation link. Hence, it is only natural to assume the PS to be either located in a GS or in a satellite outside the constellation. Details of the PS operation will be discussed in Section III.

1) Client Operation: Each satellite $k \in \mathcal{K}$ runs a process to handle all application-layer communications related to the FL training. This procedure will be designed in Section IV. Upon receiving an updated global parameter vector \mathbf{w}^n , it launches the learning procedure outlined in Algorithm 1 in a separate thread for concurrent execution. This learning procedure then computes

²While this paper is focusing on DSGD-based optimization, the extension to many other iterative distributed optimization algorithms for training ML models is straightforward.

Algorithm 1 Satellite Learning Procedure

```

1: procedure CLIENTOPT( $\mathbf{w}$ )
2:   initialize  $\mathbf{w}_k^{n,0} = \mathbf{w}^n$ ,  $i = 0$ 
3:   for  $I$  epochs do ▷  $I$  epochs of mini-batch SGD
4:      $\tilde{\mathcal{D}}_k \leftarrow$  Randomly shuffle  $\mathcal{D}_k$ 
5:      $\mathcal{B} \leftarrow$  Partition  $\tilde{\mathcal{D}}_k$  into mini-batches of size  $B$ 
6:     for each batch  $\mathcal{B} \in \mathcal{B}$  do
7:        $\mathbf{w}_k^{n,i+1} \leftarrow \mathbf{w}_k^{n,i} - \frac{\eta}{|\mathcal{B}|} \nabla_{\mathbf{w}} (\sum_{\mathbf{x} \in \mathcal{B}} f(\mathbf{x}; \mathbf{w}))$ 
8:        $i \leftarrow i + 1$ 
9:     end for
10:   end for
11:    $\mathbf{g}_k(\mathbf{w}_k^n) \leftarrow \mathbf{w}_k^{n,i} - \mathbf{w}_k^{n,0}$  ▷ Compute effective gradient
12:    $\bar{\mathbf{g}}_k(\mathbf{w}_k^n) \leftarrow \text{COMPRESSGRADIENT}(\mathbf{g}_k(\mathbf{w}_k^n))$  ▷ Apply gradient compression (e.g., sparsification)
13:   return  $D_k \bar{\mathbf{g}}_k(\mathbf{w}_k^n)$ 
14: end procedure
  
```

an update to \mathbf{w}^n based on the local data set \mathcal{D}_k . After initialization in line 2, the loss function $F_k(\mathbf{w})$ is minimized in I local epochs using permutation-based mini-batch stochastic gradient descent (SGD) in lines 3–10. Instead of directly transmitting the updated model parameters $\mathbf{w}_k^{n,i}$, the effective gradient $\mathbf{g}_k(\mathbf{w}_k^n)$ is computed in line 11. While both representation $\mathbf{w}_k^{n,i}$ and $\mathbf{g}_k(\mathbf{w}_k^n)$ are theoretically equivalent, the latter is often easier to compress. This is optionally done in line 12 by calling the procedure **COMPRESSGRADIENT**, which will be defined in Section V. Without compression, **COMPRESSGRADIENT** is simply the identity function, i.e., $\bar{\mathbf{g}}_k(\mathbf{w}_k^n) = \mathbf{g}_k(\mathbf{w}_k^n)$. In a slight modification of the usual approach, Algorithm 1 returns the compressed effective gradient scaled by D_k in line 13.

Note that the subsequent results do not rely on the explicit implementation of the SGD procedure in lines 3–10. The only requirement is that the updated model parameters can be incorporated into the global model based on effective gradients using the update rules presented in Section III. However, we will use the implementation in Algorithm 1 throughout this paper.

For the routing procedure developed in Section IV, we will require an accurate estimate of the time to run Algorithm 1. Apart from scheduling delays due to multi-task computing, the runtime directly depends on the number of processor cycles for each operation in Algorithm 1. These are hardware-dependent, deterministic, and can be determined offline before deployment [34]. First, consider a single epoch. The local data set is shuffled and divided into $\lceil \frac{D_k}{B} \rceil$ mini-batches. This process takes c_{epoch} CPU cycles per sample. Computation of the stochastic gradients requires, in total, $n_d D_k c_s$ CPU cycles, where c_s is the number of cycles to process one sample for a single dimension of \mathbf{w} . Executing the gradient step takes, per mini-batch, $n_d c_{\text{step}}$ clock cycles. Thus, one epoch requires a total of $D_k c_{\text{epoch}} + n_d D_k c_s + \lceil \frac{D_k}{B} \rceil n_d c_{\text{step}}$ CPU cycles. After I epochs,

a final gradient step taking $n_d c_{\text{step}}$ cycles is performed to compute the effective gradient. The gradient compression takes an additional c_{compress} cycles (see Section V) and is assumed zero if no compression is used. Passing the result to the communication stack takes, together with other overhead occurring due to, e.g., process setup and termination, a total of c_{os} cycles. The runtime of Algorithm 1 is

$$t_l(k) = \frac{ID_k(c_{\text{epoch}} + n_d c_s) + c_{\text{step}} n_d (I \lceil \frac{D_k}{B} \rceil + 1) + c_{\text{compress}} + c_{\text{os}}}{\nu_k}, \quad (2)$$

where ν_k is the CPU frequency at satellite k .

III. ORCHESTRATION OF SATELLITE FEDERATED LEARNING

Federated learning uses a conventional client-server architecture to orchestrate the training process. While the clients compute the stochastic gradient steps for (1), the parameter server (PS) is responsible for aggregating these gradient steps, updating the global model parameters, and distributing the updated parameter vector to the clients. In a conventional FL setup, the PS is also responsible for client scheduling, modeled as an uniform sampling of a subset of clients in each global iteration. Given that FL operates on a massive number of clients, this is equivalent to a two-stage SGD step, the first step being a client selection and the second computation. Instead, SFL operates with significantly fewer (orders of magnitude) clients and each client has a much larger share of the total data, exhibiting a non-negligible contribution to the unbiased model convergence. Hence, it is reasonable that all clients participate in every global iteration.

Connectivity towards the workers is necessary for synchronization of the training process. In SFL, the communication window from a single LEO satellite towards a ground-based PS is usually in the order of a few minutes, followed by an offline period due to Earth blockage, ranging from one orbital period up to several hours. As shown in [10], the conventional FedAvg operation of collecting all local updates before creating a new global model iteration leads to severe delays in the training process. This bottleneck can be partially mitigated by modifying FedAvg for *asynchronous* operation [10]. Compared to synchronous FL, asynchronous FL has a slower convergence speed in terms of gradient steps. For ground-orchestrated SFL without ISLs, this decrease is greatly outweighed by the reduction in the delay between gradient steps, resulting in much faster overall convergence speed, measured in wall time. Leveraging ISLs, the optimal PS operation very much depends on the PS location and resulting connectivity patterns [7]. We will introduce both orchestration approaches in a unified manner in Sections IV and V.

The actual aggregation rule at the PS is easily exchangeable as long as additivity of individual client updates holds. This broadens the contribution of Section IV, as it allows to improve the PS operation while preserving the dense connectivity patterns enabled by ISLs.

A. Synchronous Orchestration

A synchronous FL PS, exemplified by FedAvg [33], repeats the following steps until a termination criterion for the global model is met: 1) Transmit the global model parameters \mathbf{w} to the scheduled clients; 2) Wait for the clients to run Algorithm 1 and return their results; 3) Aggregate the received gradients and update the global model parameters. The difference between FL algorithms is in the computation of gradients in Algorithm 1 and the update rule in Step 3). While we focus on FedAvg here, the extension to many other algorithms is trivial.

Consider global iteration n and assume all clients are scheduled to participate in this iteration. Plain FedAvg implements the update rule $\mathbf{w}^{n+1} = \frac{1}{D} \sum_{k=1}^K D_k \mathbf{w}_k^n$, where \mathbf{w}_k^n is the updated parameter vector of client k . An equivalent update rule based on effective gradients $\mathbf{g}_k(\mathbf{w}_k^n)$, as transmitted by Algorithm 1, is

$$\mathbf{w}^{n+1} = \frac{1}{D} \sum_{k=1}^K D_k (\mathbf{w}_k^{n,i} - \mathbf{w}_k^{n,0}) + \frac{1}{D} \sum_{k=1}^K D_k \mathbf{w}_k^{n,0} = \mathbf{w}^n + \frac{1}{D} \sum_{k=1}^K D_k \mathbf{g}_k(\mathbf{w}_k^n). \quad (3)$$

A common generalization is to add a global server learning rate η_s to this update rule, i.e., $\mathbf{w}^{n+1} = \mathbf{w}^n - \eta_s \boldsymbol{\gamma}^n$, where $\boldsymbol{\gamma}^n = -\frac{1}{D} \sum_{k=1}^K D_k \mathbf{g}_k(\mathbf{w}_k^n)$ [15].

The complete algorithm for PS operation in the SFL scenario, in relation to the client update procedure in Algorithm 1, is given in Algorithm 2. This is a modified version of the delay-tolerant FedAvg implementation in [10]. It is initialized in line 2, where a set of client clusters \mathcal{C} is defined. This is required for the efficient use of ISLs in Section IV. The idea is to treat each cluster as if it were an individual user, receiving the current parameter vector only once and also delivering a single effective gradient per global iteration. For now, as well as for scenarios without ISLs, it can be assumed that satellite/client k is mapped to cluster \mathcal{C}_k , with P clusters in total. The PS maintains the training process until the sequence $\{\mathbf{w}^1, \mathbf{w}^2, \dots\}$ satisfies the termination criterion in line 3. Each iteration of this outer loop corresponds to a global iteration, counted as n . The sets \mathcal{T}^n and \mathcal{R}^n track the transmission of \mathbf{w}^n and reception of the gradient update to \mathbf{w}^n per client group, respectively. Hence, the inner loop in line 5–21 runs until updates have been received from all clusters in \mathcal{C} . This loop blocks until a satellite connects to the PS

Algorithm 2 Synchronous PS Operation

```

1: initialize global iteration  $n = 0$ , model  $\mathbf{w}^0$ ,
2:       and client clusters  $\mathcal{C} = \{\mathcal{C}_1, \mathcal{C}_2, \dots\}$ 

3: while termination criterion not met do
4:   Set  $n \leftarrow n + 1$ ,  $\mathcal{T}^n = \mathcal{R}^n = \emptyset$ ,  $\mathbf{w}^n \leftarrow \mathbf{w}^{n-1}$ 

5:   while  $|\mathcal{R}^n| < |\mathcal{C}|$  do
6:     Wait until connection from satellite  $k$ :
7:     Receive message  $m$ 
8:     Find  $p$  such that  $k \in \mathcal{C}_p$ 

9:     if  $p \notin \mathcal{T}^n$  and  $m$  is request for data then
10:      Transmit  $\mathbf{w}^{n-1}$  to satellite  $k$ 
11:      Upon successful transfer, add  $p$  to  $\mathcal{T}^n$ 
12:    else if  $p \notin \mathcal{R}^n$ 
13:      and  $m$  contains gradient update  $\gamma_p$  then
14:         $\tilde{\gamma}_p \leftarrow \text{UNCOMPRESSGRADIENT}(\gamma_p)$ 
15:         $\mathbf{w}^n \leftarrow \mathbf{w}^n + \frac{1}{D} \tilde{\gamma}_p$ 
16:        Add  $p$  to  $\mathcal{R}^n$ 
17:        Acknowledge reception to  $k$ 
18:    end if

19:    if  $|\mathcal{R}^n| < |\mathcal{C}|$  then
20:      Terminate connection
21:    end if
22:  end while
22: end while
  
```

Algorithm 3 Asynchronous PS Operation

```

1: initialize global iteration  $n = 0$ , model  $\mathbf{w}^0$ ,  $\mathcal{A} = \mathcal{B} = \emptyset$ ,
2:       and client clusters  $\mathcal{C} = \{\mathcal{C}_1, \mathcal{C}_2, \dots\}$ 

3: loop
4:   Wait until connection from satellite  $k$ :
5:   Receive message  $m$ 
6:   Find  $p$  such that  $k \in \mathcal{C}_p$ 
7:   if  $p \in \mathcal{A}$  and  $m$  contains gradient update  $\gamma_p$  then
8:      $\tilde{\gamma}_p \leftarrow \text{UNCOMPRESSGRADIENT}(\gamma_p)$ 
9:      $\mathbf{w}^n \leftarrow \mathbf{w}^n + \frac{1}{D} \tilde{\gamma}_p$ 
10:     $\mathcal{A} \leftarrow \mathcal{A} \setminus \{p\}$ 
11:    Acknowledge reception to  $k$ 
12:    Wait for new message  $m$ 

13:   if termination criterion is met then
14:      $\mathcal{B} \leftarrow \{1, 2, \dots, P\} \setminus \mathcal{A}$ 
15:     if  $\mathcal{A} = \emptyset$  then
16:       Terminate loop (and connection)
17:     end if
18:   else
19:      $\mathcal{B} \leftarrow \emptyset$ 
20:   end if
21: end if
22:   if  $p \notin \mathcal{A} \cup \mathcal{B}$  and  $m$  is request for data then
23:     Transmit  $\mathbf{w}^{n-1}$  to satellite  $k$ 
24:     Upon successful transfer, add  $p$  to  $\mathcal{A}$ 
25:   end if
26:   Terminate connection
27: end loop
  
```

in line 6. Note that this could also mean continuing a connection that was not terminated the previous iteration. A message from the satellite is received that either requests the transmission of the current parameter vector or contains the update from the satellite's cluster.

If the satellite requests transmission of \mathbf{w}^n and it was not yet delivered to its cluster, it will be transmitted in line 10. Successful reception must be acknowledged by the satellite. A possible implementation is the Bundle protocol's custody transfer [35], [36]. Then, this cluster is marked as having received the transmission in line 11. All subsequent transmission requests for \mathbf{w}^n to satellites of this cluster will be rejected by terminating the connection in line 19. If the satellite transmits an update γ_p to \mathbf{w}^n and the cluster has not yet transmitted an update in the iteration, the compression applied in line 12 of Algorithm 1 is decoded in line 13. Without compression, UNCOMPRESSGRADIENT is the identity function. Then, the update rule (3) is applied in line 14. incrementally (see also line 4) and relies on the received gradient already being scaled by D_k . Unless the current iteration is finished, the connection is terminated in Algorithm 2.

B. Asynchronous Orchestration

As opposed to synchronous operation, in asynchronous PS operation the PS does not delay the global model update until all clients have delivered their local updates. Instead, it opportunistically incorporates received gradient updates into a new iteration of the global model, which is subsequently distributed to the clients. Consequently, clients simultaneously operate on different version of the model parameters and gradient updates are typically based on an outdated version of the model parameters, reducing the convergence speed and, potentially, numerical problems. For SFL, this *staleneness*, i.e., the age of the local model with respect to the current global model, is bounded due to the quasiperiodicity of this scenario. Hence, we are operating in the partially asynchronous domain, which leads to, generally speaking, much better convergence properties than in totally asynchronous scenarios with unbounded delays [37].

Inspired by [10], an asynchronous version of Algorithm 2 is proposed in Algorithm 3. It consists of the same functional blocks as Algorithm 2: Wait for incoming connections in lines 4–6, incorporate and acknowledge gradient updates in lines 8–11, run until global convergence (lines 13–21), and transmit the current version of the model parameters in lines 23–24. The main difference is that, in Algorithm 2, the nested loop ensures that every cluster adds their update to the global model before this new version is transmitted to any client. Instead, Algorithm 3 directly incorporates every received update and immediately starts using this new version to answer requests for data. To avoid race conditions within the clusters, Algorithm 3 uses the set \mathcal{A} to track active clusters, i.e., clusters that received the model parameters and did not yet return an update. Another difference is that the global termination criterion, after being first met, might not remain valid after receiving the outstanding updates from active clusters. To handle this, whenever a new global model satisfies the termination criterion, all inactive clusters in \mathcal{B} , including the currently connected, are blocked from further computations. This is repeated until no active cluster remains. If the termination criterion is violated for any update, all blocks are removed in line 19 and the algorithm resumes normal operation.

IV. INTRA-ORBIT AGGREGATION FOR SATELLITE FL

Convergence in SFL is mainly impaired by the connectivity bottleneck between satellites and the PS. We have discussed algorithmic approaches to this obstacle in the previous section. With the availability of ISLs, these can be complemented by multi-hop routing to close gaps in connectivity. Figure 2 illustrates the potential gain for a constellation having five orbital planes,

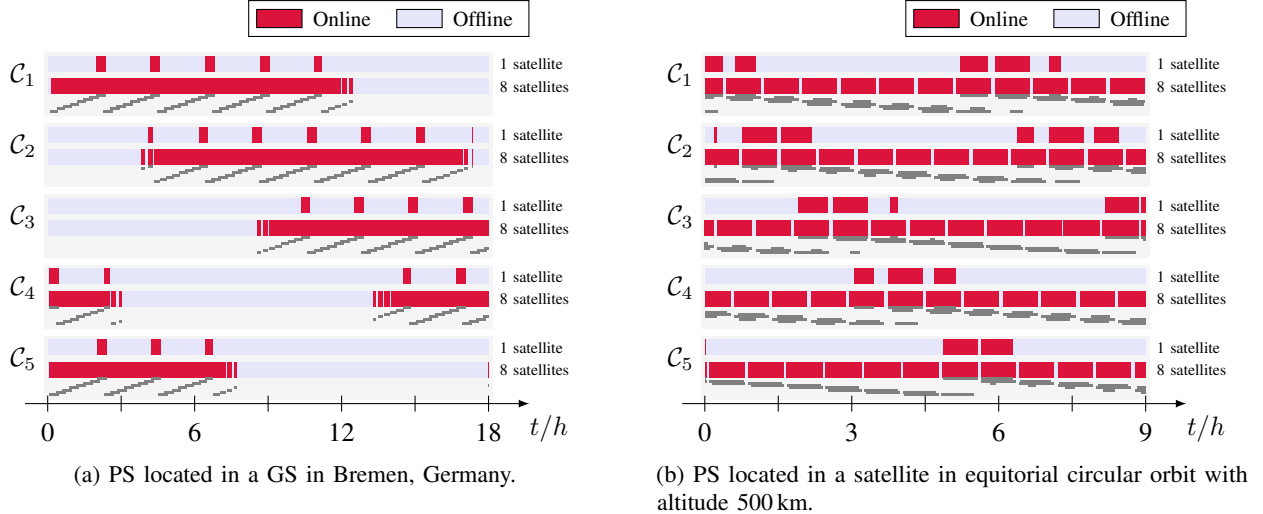


Fig. 2. Connectivity towards the PS from within a 60° : 40/5/1 Walker delta constellation. That is, a constellation of 40 satellites having 60° inclined circular orbits and altitude 2000 km. The satellites are distributed evenly among five orbital planes, which are spaced equidistantly around Earth. Clusters \mathcal{C}_p are defined as either a single satellite per orbital plane or all satellites within an orbital plane. In the second case, a cluster is considered having a connection to the PS if at least one satellite of the cluster can communicate with the PS. Per-satellite connectivity towards the PS is displayed in gray below the cluster connectivity.

each with eight satellites, displaying the connection of a single satellite from each plane towards a PS. Using multi-hop routes within the orbital plane leads to significantly prolonged online periods as compared to the sporadic point-to-point connectivity. For simplicity, we focus on synchronous orchestration first and review the specifics for asynchronous orchestration in Section IV-F.

Communication for FL involves two primary tasks, parameter vector distribution and collection of gradient updates. A direct approach to implementing these, leveraging ISLs for multi-hop routing, are conventional delay-tolerant networking (DTN) techniques for satellite networks, e.g., contact graph routing in combination with the Bundle protocol [38]–[40]. Then, parameter vector distribution is a multicast message from the PS towards all satellites in \mathcal{K} , while gradient updates are communicated as unicast messages from individual satellites towards the PS. However, the number of these unicast transmissions scales quadratically in the number of satellites per orbital plane. This can be reduced to a linear increase with in-network aggregation.

A. Incremental Aggregation

Consider the PS update rule from (3), within the global iteration n . The PS is primarily interested in the sum of effective gradients instead of individual gradient updates. Hence, the updates from all satellites within an orbital plane \mathcal{K}_p can be collected at a single satellite $s_p^n \in \mathcal{K}_p$ for transmission

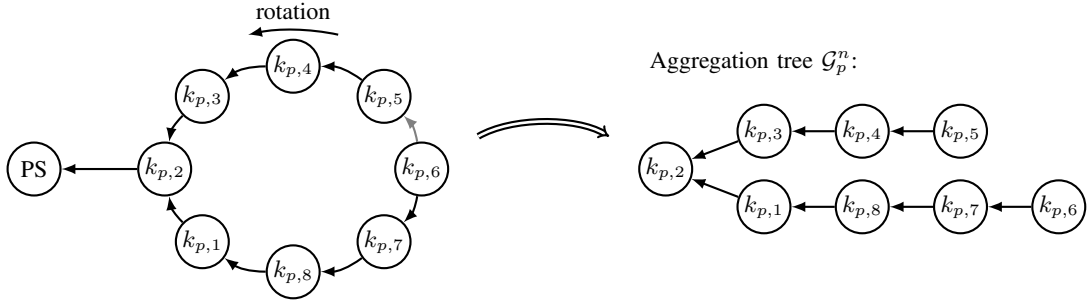


Fig. 3. Routing tree for incremental aggregation in orbital plane p . Satellite $k_{p,2}$ acts as sink node. Satellite $k_{p,6}$ has two shortest-path routes to sink. This is resolved unambiguously by the routing algorithm.

to the PS. Instead of transmitting the individual gradient updates $\{D_k \bar{\mathbf{g}}_k(\mathbf{w}_k^n)\}_{k \in \mathcal{K}_p}$, this satellite sends the linear combination $\sum_{k \in \mathcal{K}_p} D_k \bar{\mathbf{g}}_k(\mathbf{w}_k^n)$ to the PS. Following Section III, the PS then treats the satellites in \mathcal{K}_p as the client cluster \mathcal{C}_p and incorporates their joint update.

This approach can be extended to intra-cluster communication. Suppose the sink satellite s_p^n is known to all satellites in \mathcal{K}_p . Then, each satellite can easily determine a shortest-path in-tree, rooted at and oriented towards s_p^n , for \mathcal{K}_p [41, §9.6]. For K_p odd, this tree is unique. For K_p even, two equal length paths exist for the satellite farthest away from s_p^n . Denote this satellite $k_{p,i}$ and resolve this ambiguity by choosing the tree where $k_{p,i+1}$ is the parent node of $k_{p,i}$. We denote this directed graph as the *aggregation tree* $\mathcal{G}_p^n = (\mathcal{K}_p, \mathcal{E}_p^n)$, with vertex set \mathcal{K}_p and edge set \mathcal{E}_p^n . Its computation is illustrated in Figure 3.

Let $\mathcal{N}_{\mathcal{G}_p^n}^-(k) = \{y \in \mathcal{K}_p : (y, k) \in \mathcal{E}_p^n\}$ be the incoming neighborhood of k on \mathcal{G}_p^n . Based on \mathcal{G}_p^n , each satellite $k \in \mathcal{K}_p$ knows exactly which gradient updates it needs to forward. After local computation completes, node k waits until all updates from the satellites in $\mathcal{N}_{\mathcal{G}_p^n}^-(k)$ are received via ISLs. This might have already happened during the local computation phase. Then, the outgoing partial aggregate of satellite k is computed as

$$\gamma_k^n = D_k \bar{\mathbf{g}}_k(\mathbf{w}_k^n) + \sum_{y \in \mathcal{N}_{\mathcal{G}_p^n}^-(k)} \gamma_y^n \quad (4)$$

and transmitted via ISL to the next hop $p \in \mathcal{N}_{\mathcal{G}_p^n}^+(k) = \{y \in \mathcal{K}_p : (k, y) \in \mathcal{E}_p^n\}$. If k is the current³ sink node, i.e., $|\mathcal{N}_{\mathcal{G}_p^n}^+(k)| = 0$, γ_k^n is the joint aggregate of client cluster $\mathcal{C}_p = \mathcal{K}_p$ and transmitted to the PS once the link becomes available.

³Please refer to Section IV-D for a failure handling procedure that might change the sink node after initial assignment.

B. Parameter Vector Distribution

Algorithms 2 and 3 treat client clusters as if they were a single node, i.e., the PS expects to receive a single (joint) update per client cluster and transmits the model parameter vector only once per global iteration to each cluster. The previous subsection provides ample reason for the first design choice. Transmitting the parameter vector only once is also sensible for several reasons. First of all, it is what ideally happens if the PS transmits a multicast message towards the nodes in \mathcal{K}_p using the Bundle protocol. As noted before, using the Bundle protocol's custody transfer (or similar) to safeguard point-to-point transmissions involving the PS is a fundamental assumption in this paper. Second, using multicast messages and multi-hop routing considerably reduces delay and the communication effort for the PS. Finally, this provides a natural leader election mechanism for coordinating the sink node selection.

The PS sends the model parameters \mathbf{w}^n in iteration n to a single satellite k per cluster \mathcal{C}_p . Satellite k is then responsible for determining an appropriate sink node s_p^n using the procedure described in Section IV-C. Subsequently, satellite k propagates its routing decision together with \mathbf{w}^n through both ISLs to its neighbors $\mathcal{N}(k)$ and starts the local training $\text{CLIENTOPT}(\mathbf{w}^n)$. All other satellites, upon reception of new model parameters \mathbf{w}^n via one of the ISLs, forward the model parameters to their next neighbor that did not receive \mathbf{w}^n and start the local training $\text{CLIENTOPT}(\mathbf{w}^n)$. Subsequent receptions of \mathbf{w}^n are silently dropped upon reception. This ensures that the propagation of \mathbf{w}^n through the orbital plane stops once every satellite received it.

C. Predictive Routing

The final missing piece to this routing approach is a procedure to determine the sink node s_p^n . This decision must be made before the local training procedure completes on any satellite in the client cluster. From a timing perspective, the ideal sink node completes computing (4) immediately before its link towards the PS becomes available. Predicting the future state of a satellite constellation is possible with high accuracy due to the determinism of satellite movement [42]–[44]. Here, we assume the availability of an orbital propagator with low computational complexity and (relatively) low precision like SGP4 [43], [45]. We also assume availability of fairly recent information on the constellation state, e.g., in the form of two-line element sets (TLEs) [45], [46], distributed by the satellite operator. The sink node can be determined from the orbital positions of the PS and satellites \mathcal{K}_p at the time when intra-orbit aggregation completes. This requires a prediction of the time T_p^n to 1) distribute the model parameters; 2) compute the

local updates; and 3) deliver these updates to candidate sink nodes. The computation time can be estimated using $t_l(k)$ in (2). The time to transmit a vector \mathbf{v} via intra-orbit ISL between two satellites k_1 and $k_2 \in \mathcal{N}(k_1)$ is upper bounded as $t_c(\mathbf{v}, t; k_1, k_2) \leq \frac{S(\mathbf{v})}{\rho_{k_1, k_2}} + \frac{\max_t d(t; k_1, k_2)}{c_0}$, where c_0 is the vacuum speed of light, $S(\mathbf{v})$ is the storage size of \mathbf{v} and $d(t; k_1, k_2)$ is constant in t for circular orbits. For uncompressed gradients, $S(\mathbf{w}^n) = n_d \omega$, where ω is the storage size of a single element of model parameter, usually 16-bit or 32-bit floating point number.

A precise solution for T_p^n should take into account that satellites start their learning procedure at different times depending on the number of hops the global model parameters need to travel. Even when distribution takes place over shortest-distance paths, the completion time is different for each potential sink node in \mathcal{K}_p . Hence, predictions on the constellation state must be made for up to K_p time instants and the computational complexity for determining the sink node scales at least linearly in K_p . A considerably simpler approach is to assume distribution takes place over shortest-distance paths and make a worst-case estimate for the aggregation phase. Combined with assuming a symmetric orbital distribution of satellites and equal ISL capabilities, i.e., $d_p = \max_t d(t; k_1, k_2)$ and $\rho_p = \rho_{k_1, k_2}$ for all $k_1 \in \mathcal{K}_p, k_2 \in \mathcal{N}(k_1)$, we obtain

$$T_p^n \leq \left\lceil \frac{K_p}{2} \right\rceil \left(\frac{S(\mathbf{w}^n)}{\rho_p} + \frac{d_p}{c_0} \right) + \max_{k \in \mathcal{K}_p} t_l(k) + \left\lceil \frac{K_p}{2} \right\rceil \left(\frac{\max_{k \in \mathcal{K}_p} S(\bar{\mathbf{g}}_k(\mathbf{w}_k^n))}{\rho_p} + \frac{d_p}{c_0} \right). \quad (5)$$

Under constant-length gradient compression and equal in-cluster computation times, becomes:

$$T_p^n \leq \hat{T}_p^n = t_l(k_1) + \left\lceil \frac{K_p}{2} \right\rceil \left(\frac{S(\mathbf{w}^n) + S(\bar{\mathbf{g}}_{k_1}(\mathbf{w}_{k_1}^n))}{\rho_p} + \frac{2d_p}{c_0} \right) \quad (6)$$

for any $k_1 \in \mathcal{K}_p$. This bound overestimates the time for communications. However, this part is likely small compared to the computation time. Taking into account the inaccuracies of orbital prediction,⁴ local clock deviations, and computational delays due to, e.g., multitasking, interrupts, or priority scheduling, slightly overestimating the time to completion seems reasonable. The major advantage of using the simple estimate in (6) is that the constellation state needs only be predicted for a single time instant. Thus, the computational effort remains constant in K_p .

Based on the estimate \hat{T}_p^n , the satellite that took custody of \mathbf{w}^n computes the positions of the PS and all satellites in its orbital plane at time $t_p^n + \hat{T}_p^n$, where t_p^n is the expected local time after determining s_p^n . It then selects the satellite with the shortest Euclidean distance to the PS as sink node s_p^n and starts the model distribution (cf. Section IV-B).

⁴TLE data has an initial accuracy of roughly 1 km and then decays quickly [45].

D. Failure Handling

The most critical routing error occurs if the sink node completes incremental aggregation directly after its communication window to the PS has closed. This could introduce large delays with significant impact on the global FL process. The straightforward mitigation approach is to use conventional DTN multi-hop routing to deliver the cluster update to the PS. However, this is unnecessary if the sink node token is passed once the designated communication window closes. Specifically, upon receiving the model parameters, the sink node $s_p^n = k_{p,i}$ determines the predicted time of completion for incremental aggregation as

$$T_c = t + t_l(s_p^n) + \left\lceil \frac{K_p}{2} \right\rceil \left(\frac{S(\bar{\mathbf{g}}_{s_p^n}(\mathbf{w}_{s_p^n}^n))}{\rho_p} + \frac{2d_p}{c_0}, \right) \quad (7)$$

where t is the current (local) time, and the PS communication window such that $T_c \in [t_1, t_2]$. After time t_1 , the sink node actively monitors the link towards the PS and, upon detecting the closure of the communication window, it passes the sink node role to its neighbor $k_{p,i+1}$. Then, satellites $k_{p,i}$ and $k_{p,i+1}$ update their aggregation trees and start normal operation in their new role. The new sink takes t_1 as the current time, the old sink checks whether it can compute and forward (4), while the other satellites in \mathcal{K}_p do not need to be informed of this change.

E. Algorithm

The satellite operation described above is summarized in Algorithm 4. This procedure runs until a stop message is received from the PS, either directly or via ISL. The parameter vector distribution is handled in lines 3–19. Lines 7–9 are for failure handling and move the satellite back into the aggregation phase to take over the sink node role. The training procedure is launched concurrently, e.g., in a separate thread, in line 20. Algorithm 4 continues immediately with line 21, which starts the incremental aggregation phase by computing \mathcal{G}_p^n .

If the satellite is the current sink node, it waits for incoming results and its own computation to finish. Should the designated PS communication window pass in the meantime, an interrupt is generated according to the procedure described in Section IV-D. It triggers the handover procedure in lines 26–28, which passes the sink node token and restarts the local aggregation phase. Otherwise, once all results are ready, the sink node computes the final cluster aggregate in line 30, waits for the PS to become available, and transmits the results.

Algorithm 4 Satellite Operation

```

1: Initialize global iteration  $n = 0$ , satellite ID  $k = k_{p,i}$ 
2: and orbital plane ID  $p$ 
3: Wait for incoming ISL or start of PS connectivity window
4: if received  $(s_p^{n+1}, \mathbf{w}^{n+1})$  from satellite  $l$  then
5:    $n \leftarrow n + 1$ 
6:   Forward  $(s_p^n, \mathbf{w}^n)$  to  $\mathcal{N}(k) \setminus \{l\}$ 
7: else if received sink token from satellite  $l$  then
8:   Set  $t_1$  to current time and update  $s_p^n \leftarrow k$ 
9:   Goto line 21
10: else if connected to PS then
11:   Request parameters  $\mathbf{w}^{n+1}$  and wait for reply
12:   if received  $\mathbf{w}^{n+1}$  then
13:     Acknowledge reception to PS and set  $n \leftarrow n + 1$ 
14:     Compute  $t_p^n + \hat{T}_p^n$  and determine  $s_p^n$ 
            $\triangleright$  cf. Section IV-C
15:     Transmit  $(s_p^n, \mathbf{w}_p^n)$  to  $\mathcal{N}(k)$ 
16:   else
17:     Goto line 3
18:   end if
19: end if
20: Execute concurrently  $D_k \bar{g}_k(\mathbf{w}_k^n) \leftarrow \text{CLIENTOPT}(\mathbf{w}^n)$ 
21: Compute aggregation tree  $\mathcal{G}_p^n$   $\triangleright$  cf. Section IV-A
22: if  $k$  is sink satellite then
23:   Initialize handover interrupt  $\triangleright$  cf. Section IV-D
24:   Wait for [ CLIENTOPT and results from  $\mathcal{N}_{\mathcal{G}_p^n}^-(k)$  ]
           until handover interrupt
25:   if handover interrupt then
26:     Pass sink token to  $k_{p,i+1}$ 
27:     Update  $s_p^n \leftarrow k_{p,i+1}$ 
28:     Goto line 21
29:   else
30:     Compute  $\gamma_k^n$  as in (4)
31:     Wait for connection to PS
32:     Transmit  $\gamma_k^n$  and wait for acknowledgement
33:   end if
34:   else
35:     Wait for [ CLIENTOPT and results from  $\mathcal{N}_{\mathcal{G}_p^n}^-(k)$  ]
           or sink token
36:     if sink token then
37:       Set  $t_1$  to current time and update  $s_p^n \leftarrow k$ 
38:       Goto line 21
39:     else
40:       Compute  $\gamma_k^n$  as in (4)
41:       Transmit  $\gamma_k^n$  to next hop  $p \in \mathcal{N}_{\mathcal{G}_p^n}^+(k)$ 
42:     end if
43:   end if
44: Goto line 3
  
```

All other satellites execute lines 34–43. If the local training is complete and the expected incoming partial aggregate is received, the satellite computes (4) and forwards the result to the next hop in line 41. It then returns to line 3 to wait for a new global iteration or take over as sink node. If the satellite is tasked with taking over as sink node, it updates the relevant parameters in line 37 and restarts the aggregation phase.

F. Asynchronous Orchestration

The primary reason for asynchronous orchestration is long connectivity gaps due to orbital mechanics. These outages are considerably reduced by the techniques developed in this section. As there is no apparent benefit of per-client asynchronous updates over using (synchronous) client clusters, the system performance under asynchronous aggregation is expected to benefit significantly from incremental intra-orbit aggregation. In fact, the proposed FL system can be implemented such that the clients are agnostic to the PS operation.

However, in some scenarios the improved connectivity can result in a large number of updates from a small group of client clusters. This can lead to heavily biased solutions and other convergence issues. One such problematic scenario could be Fig. 2b combined with a short learning time $t_l(k)$. A simple solution to this issue is to set a maximum update frequency

per cluster, i.e., fix a minimum time T_u between updates. In a completely trusted system (as is likely the case in SFL), this can be implemented by 1) modifying line 14 in Algorithm 4 to use $\max\{\hat{T}_p^n, T_u\}$ instead of \hat{T}_p^n ; 2) distributing the time stamp $t_p^n + T_u$ together with the model parameters and designated sink node; and 3) not sending any updates to the PS before $t_p^n + T_u$, unless this would result in missing the planned communication window (modify line 31 in Algorithm 4). Alternatively, the PS could simply refuse sending the current global model parameters to a cluster if the update frequency is too high.

V. SPARSIFICATION-BASED GRADIENT COMPRESSION

Synchronizing large-scale ML models requires transmitting massive amounts of data. A widely employed method to reduce the communication cost is to truncate the effective gradients prior to transmission to only contain the elements with largest magnitude, while setting the other elements to zero. This is known as *sparsification* [47], [48], as the resulting vectors are communicated in sparse vector encoding. With practical sparsification ratios q in the range of 1 % to 10 %, the size of a single effective gradient vector can be reduced by approximately 80 % to 98 %.

However, while a single sparsified vector has a deterministic length of $\lfloor n_d q \rfloor$ nonzero elements, the sum of multiple sparse length- $\lfloor n_d q \rfloor$ vectors has nondeterministic length. This leads to variable transmission lengths and, hence, uncertainties in the predictive routing procedure. In this section, we develop an estimator for sparse vectors subject to incremental aggregation based on probabilistic modeling of the weight vectors. Before, we briefly review FL gradient sparsification.

A. Gradient Sparsification for FL

Each client transmits only the $\lfloor n_d q \rfloor$ largest magnitude elements from its effective gradient vector $\mathbf{g}_k(\mathbf{w}_k^n)$. This truncation operation is denoted as Top_q . A common method to improve the training performance under gradient sparsification is to track the accumulated sparsification error in a residual vector Δ_k^n . The effect is that small magnitude elements, which would be ignored in every iteration, are aggregated over several iterations and will survive sparsification at some point.

The complete sparsification procedure, for an effective gradient $\mathbf{g}_k(\mathbf{w}_k^n)$, is to accumulate the previous sparsification error into the effective gradient as $\mathbf{g}_k^{\text{acc}}(\mathbf{w}_k^n) \leftarrow \mathbf{g}_k(\mathbf{w}_k^n) + \Delta_k^{n-1}$, then compute the sparse gradient for transmission as $\bar{\mathbf{g}}_k(\mathbf{w}_k^n) \leftarrow \text{Top}_q(\mathbf{g}_k^{\text{acc}}(\mathbf{w}_k^n))$, and update the

sparsification error as $\Delta_k^n \leftarrow \mathbf{g}_k^{\text{acc}}(\mathbf{w}_k^n) - \bar{\mathbf{g}}_k(\mathbf{w}_k^n)$. Convergence of SGD with this sparsification procedure is established in [48]. The COMPRESSGRADIENT procedure in Algorithm 1 is implemented as exactly these three steps, with $\bar{\mathbf{g}}_k(\mathbf{w}_k^n)$ being the return value. Then, UNCOMPRESSGRADIENT simply converts the sparse vector back to its full-length representation, and the summation in (4) is implemented as a conventional sparse vector addition [49, §2].

B. Predictive Routing for Sparse Incremental Aggregation

The predictive routing procedure in Section IV-C relies on knowledge of the storage size $S(\bar{\mathbf{g}}_k(\mathbf{w}_k^n))$. With sparsification applied, the estimates in (6) and (7) remain no longer valid. Indeed, the relevant length is $S(\boldsymbol{\gamma}_k^n)$ which is no longer constant over the aggregation path. To this end, first consider the following lemma.

Lemma 1: Consider L independent and identically distributed (i.i.d.) random vectors $\mathbf{X}_1, \dots, \mathbf{X}_L$ of dimension n_d . Let $\tilde{\mathbf{X}}_l = \text{Top}_q(\mathbf{X}_l)$ for all $l = 1, \dots, L$. Then, the expected number of nonzero elements in $\mathbf{X}_\Sigma = \sum_{l=1}^L \tilde{\mathbf{X}}_l$ is $n_d - n_d \left(1 - \frac{n_a}{n_d}\right)^L$, where $n_a = \lfloor n_d q \rfloor$ is the number of nonzero elements in each summand.

Proof: Consider the vector $\mathbf{X}_l = (X_{l,1}, \dots, X_{l,n_d})$ and let $A_{l,i}$ be the event that $X_{l,i}$ is zero after the Top_q operation. The probability that $A_{l,i}$ occurs is $1 - \frac{n_a}{n_d}$ [50, Lemma 13.1]. Further, let A_i be the event that element i is zero after Top_q in all L vectors. Then, due to independence, $\Pr(A_i) = \Pr\left(\bigcap_{l=1}^L A_{l,i}\right) = \prod_l \Pr(A_{l,i}) = \left(1 - \frac{n_a}{n_d}\right)^L$. Observe that A_i is the event that the i th element of \mathbf{X}_Σ is zero. Thus, the expected number of zero elements in \mathbf{X}_Σ is $\mathbb{E}[\sum_{i=1}^{n_d} I(A_i)] = \sum_i \mathbb{E}[I(A_i)] = \sum_i \Pr(A_i) = n_d \left(1 - \frac{n_a}{n_d}\right)^L$, where $I(\cdot)$ is the indicator function that takes value 1 if A_i occurs and 0 otherwise. ■

Based on this lemma, we can make a reasonable estimate on the number of transmitted bits during incremental aggregation.

Proposition 1: The expected total number of transmitted bits over H hops of incremental aggregation is upper bounded as $n_d(\omega + \lceil \log_2 n_d \rceil) \left[H + 1 - \frac{n_d}{n_a} \left[1 - \left(1 - \frac{n_a}{n_d}\right)^{H+1} \right] \right]$, where $n_a = \lfloor n_d q \rfloor$.

Proof: Let $P_h = (k_1, k_2, \dots, k_{h+1})$, for $h = 1, 2, \dots, H$, be an increasing sequence of nested paths. Consider incremental aggregation over path P_H starting at k_1 . Denote by $S(P_h)$ the total number of bits transmitted over path P_h . Then, $S(P_1) = S(\boldsymbol{\gamma}_{k_1}^n)$ and $S(P_h) = S(\boldsymbol{\gamma}_h^n) + S(P_{h-1})$ for $h > 1$, where $\boldsymbol{\gamma}_k^n$ is the outgoing aggregate at node k as defined in (4). At k_1 , the outgoing

aggregate has storage size $S(\boldsymbol{\gamma}_{k_1}^n) = n_a(\omega + \lceil \log_2 n_d \rceil)$, where $\lceil \log_2 n_d \rceil$ accounts for the storage space of element indices in the sparse representation [49, §2].

At subsequent nodes k_h , $h > 1$, the outgoing aggregate has size $S(\boldsymbol{\gamma}_{k_h}^n) = S(D_{k_h} \bar{\mathbf{g}}_{k_h}(\mathbf{w}_{k_h}^n) + \boldsymbol{\gamma}_{k_{h-1}}^n)$. Modelling \mathbf{w}_k^n as an i.i.d. random vector and assuming the gradients of the nodes along P_H are independent, we obtain $\mathbb{E}[S(\boldsymbol{\gamma}_{k_h}^n)] = (\omega + \lceil \log_2 n_d \rceil) \left(n_d - n_d \left(1 - \frac{n_a}{n_d}\right)^h \right)$ from Lemma 1. Further, observe that $S(\boldsymbol{\gamma}_{k_1}^n) = n_d - n_d \left(1 - \frac{n_a}{n_d}\right)$. Then, by recursion, $\mathbb{E}[S(P_H)] = \sum_{h=1}^H \mathbb{E}[S(\boldsymbol{\gamma}_h^n)] = n_d(\omega + \lceil \log_2 n_d \rceil) \left[H - \sum_{h=1}^H \left(1 - \frac{n_a}{n_d}\right)^h \right]$, and due to the geometric sum identity, $\mathbb{E}[S(P_H)] = n_d(\omega + \lceil \log_2 n_d \rceil) \left[H + 1 - \frac{n_d}{n_a} \left(1 - \left(1 - \frac{n_a}{n_d}\right)^{H+1}\right) \right]$.

Finally, observe that for dependent gradients the positions of the nonzeros after Top_q will be correlated. Hence, with the notation from the proof of Lemma 1, $\Pr(A_{l,i}) \leq \Pr(A_{l,i} | A_{l,i-1} \dots A_{l,1})$. Thus, $\Pr(A_i) \geq \left(1 - \frac{n_a}{n_d}\right)^L$ and $\mathbb{E}[\sum_i I(A_i)] \geq n_d \left(1 - \frac{n_a}{n_d}\right)^L$. \blacksquare

Leveraging Proposition 1, we replace $\left\lceil \frac{K_p}{2} \right\rceil S(\bar{\mathbf{g}}_{k_1}(\mathbf{w}_{k_1}^n))$ in (6) and (7) with

$$n_d(\omega + \lceil \log_2 n_d \rceil) \left[\left\lceil \frac{K_p}{2} \right\rceil + 1 - \frac{n_d}{n_a} \left[1 - \left(1 - \frac{n_a}{n_d}\right)^{\left\lceil \frac{K_p}{2} \right\rceil + 1} \right] \right], \quad (8)$$

to account for sparsification in the predicted routing procedure. This will overestimate the communication effort as it does not account for the dependence between gradients. However, a tighter bound would require assumptions on a random distribution for elements of \mathbf{w} and experimental calibration of correlation between gradients. If this precision is required, the measured data could also be used to directly train a simple ML estimator for the aggregated vector length.

VI. PERFORMANCE EVALUATION

We evaluate the performance of the proposed system design for four representative scenarios. The worker satellites are organized either in a 60° : 40/5/1 Walker Delta or a 85° : 40/5/1 Walker star constellation, both at an altitude of 2000 km. The notation $i:t/p/f$ indicates a constellation with p evenly spaced circular orbital planes at inclination i , each having t/p equidistant satellites. The phasing parameter f defines the relative shift in right ascension of the ascending node between adjacent orbital planes and amounts to 9° in this particular setup [51]. Subsequently, we identify these constellations as W- Δ and W- \star , respectively. These constellations are combined with a PS located either in a terrestrial GS located in Bremen, Germany, or in a LEO satellite orbiting at an altitude of 500 km in the equatorial plane.

Communication links are modelled as complex Gaussian channels with free-space path loss (FSPL). Then, the maximum achievable rate between nodes k and i using a bandwidth B is $\rho(k,i) = B \log_2 (1 + \text{SNR}(k,i))$. The $\text{SNR}(k,i) = \frac{P_t G_k(i) G_i(k)}{N_0 L(k,i)}$ is defined by the transmit power P_t , the noise spectral density $N_0 = k_B T B$ at receiver temperature T , and average antenna gains $G_j(l)$ at node j towards node l , with k_B being the Boltzmann constant. The FSPL is $L(k,i) = (4\pi f_c d(k,i)/c_0)^2$, where f_c is the carrier frequency and $d(k,i)$ the distance between nodes k and i [32], [52]. We assume fixed rate links operating at the minimum rate supported by the link. This is equivalent to selecting $d(k,i)$ as the maximum communication distance $d_{\text{Th}}(k,i)$ between these nodes. Following [51], we set $f_c = 20$ GHz, $B = 500$ MHz, $P_t = 40$ dBm, $T = 354$ K, and the antenna gains to 32.13 dBi.

Numerical ML performance is evaluated based on the two most widely used benchmarks. The first is a conventional 7850-parameter logistic regression model trained on the MNIST dataset, 28×28 pixel greyscale images of handwritten digits ranging from 0 to 9 [53]. The other is a deep CNN with 122 570 parameters from [54], trained on the CIFAR-10 dataset [55], which includes 10 classes with 32×32 RGB images. The data samples are either evenly distributed at random among the satellites, which is the i.i.d. setting, or in a non-i.i.d. fashion using a Dirichlet distribution with parameter 0.5 [56], [57]. We use a batch size of ten, run five local epochs, and take the learning rate as 0.1. A computation time t_l of 60 s and 480 s is assumed for MNIST and CIFAR-10, respectively. The simulation is build upon the FedML framework [58].

A. Synchronous and Asynchronous Orchestration

We start by evaluating the benefits of ISLs for synchronous orchestration as detailed in Algorithm 2. Without employing ISLs, this is the vanilla FL approach as first proposed in [33]. Directly applying it to SFL, i.e., each satellite contacts the PS directly, leads to very slow convergence speed, especially in scenarios with terrestrial orchestration [10]. The question is whether the usage of ISLs resolves the connectivity bottleneck sufficiently to make synchronous orchestration feasible.

To this end, we measure the test accuracy with respect to the wall clock time for synchronous terrestrial orchestration in the W- \star and W- Δ constellations, with and without ISLs. We complement this by an experiment with a PS in LEO. Results for non-i.i.d. MNIST and CIFAR-10 are displayed in Fig. 5. All scenarios show the distinct step function behavior first observed in [10] for the non-ISL scenarios. This is caused by the PS being forced to wait for all results before updating

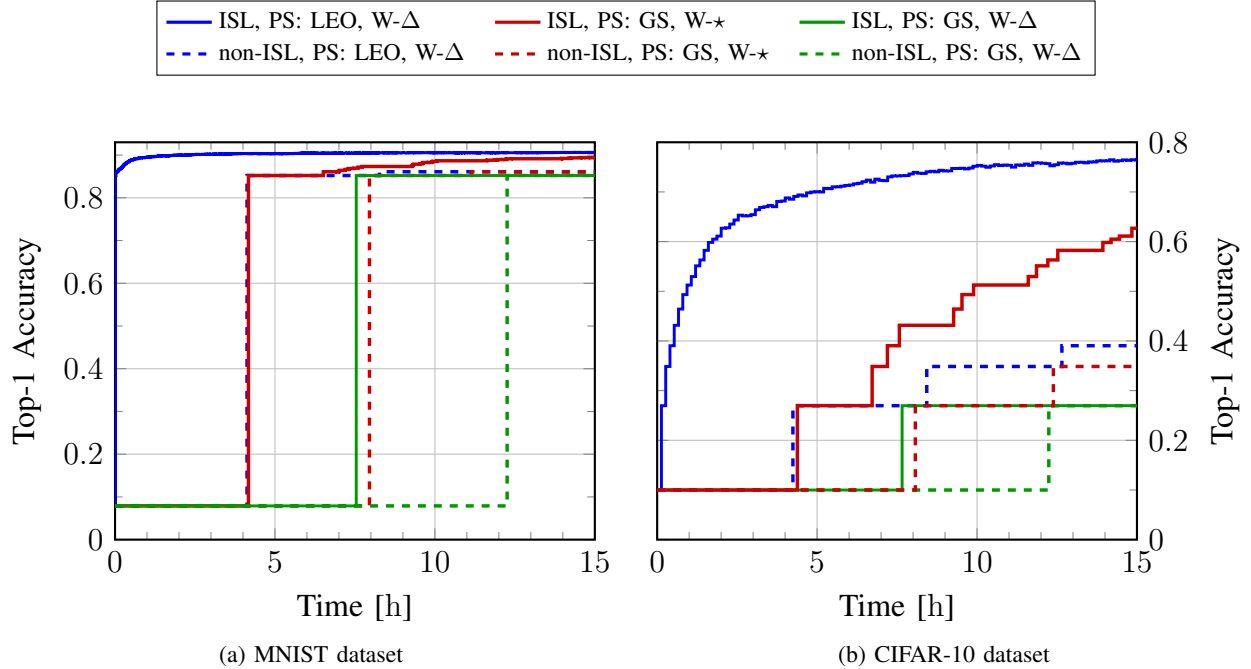


Fig. 4. Test accuracy with respect to wall-clock time. Synchronous orchestration for the MNIST and CIFAR-10 datasets with non-i.i.d. distributions, considering both terrestrial and non-terrestrial PS, i.e., the GS in Bremen and an LEO satellite. Note that ISL and non-ISL stand for the FedAvg with and without ISL algorithms respectively.

the global model. As expected, the usage of ISLs, as proposed in Section IV, shortens the convergence time significantly in all scenarios. With MNIST training usually showing very fast convergence, it can be easily observed that ISLs reduce the time to convergence in all scenarios by 4 hours. This leads to almost instantaneous convergence in the LEO scenario, at least in relation to the training duration in conventional SFL, and reduces the convergence time by up to 50 % for terrestrial orchestration.

The CIFAR-10 experiment was chosen to evaluate the convergence behavior of a more involved ML model. As such, convergence requires a large number of global iterations. From Fig. 4b, we observe a more nuanced convergence behavior as compared to the MNIST experiment. In particular, LEO-based orchestration benefits most from ISLs, while W- Δ profits only in the initial learning phase. Surprisingly, it basically shows the same convergence speed as without ISLs, simply shifted in time by a few hours. The reason behind this is best understood from Fig. 2, which displays exactly the connectivity patterns of these two scenarios. Connectivity in the LEO PS scenario changes from a sporadic towards a near-persistent connectivity pattern. Instead, for terrestrial orchestration, the connectivity windows grow significantly in duration, but the overall connectivity pattern is still sporadic. That is, the offline periods of individual orbital groups still

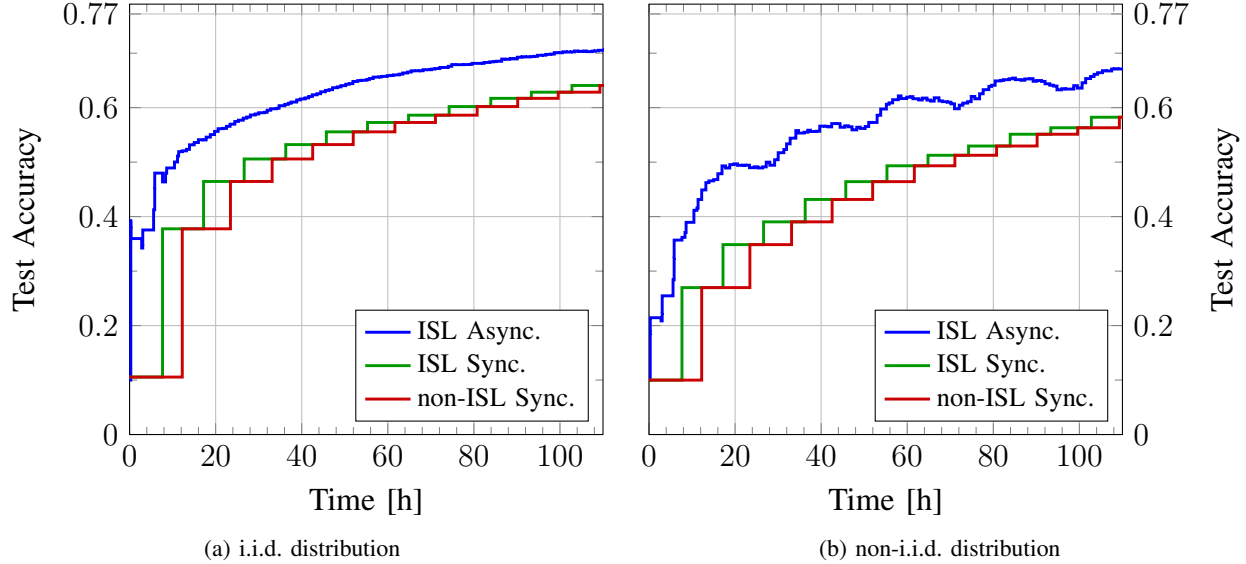


Fig. 5. Test accuracy with respect to wall-clock time for W- Δ Constellation. Synchronous and asynchronous orchestrations for the CIFAR-10 dataset with i.i.d. and non-i.i.d. distributions are included, where the PS is located in Bremen.

lead to blocking in synchronous aggregation algorithms. However, this behavior is not universal to terrestrial orchestration. It depends on the constellation design and GS location, as can be seen by the improved convergence speed in the W- \star scenario. Moreover, combining synchronous orchestration and ISLs with the scheduling approach from [19] is expected to alleviate this problem in training scenarios with limited computational complexity.

Following the discussion in Section III and [7], a viable alternative to synchronous orchestration in sporadic connectivity scenarios is asynchronous PS operation. This is evaluated in Fig. 5 for W- Δ with terrestrial orchestration, with maximum time between updates T_u set to 147 minutes. Convergence with asynchronous aggregation is improved over synchronous operation, but still involves at least a ten-fold increase in convergence time. Especially initial convergence speed, i.e., within the first few hours of training, is greatly increased. This leads to the conclusion that asynchronous aggregation is a potential solution if the system design suffers from sporadic connectivity. However, if changing the PS location is an option, it might be preferable to asynchronous orchestration.

B. Gradient Sparsification and Transmission Load

Fig. 6 shows the transmission load required for collecting the gradients in one orbit and sending them toward the PS, within a single global iteration. The results are based on the MNIST

dataset with non-i.i.d. distribution. The figure depicts the total transmitted data as a function of the number of satellites in an orbit. The total transmitted data in FedAvg with ISL algorithm are compared for two different cases, with and without incremental aggregation (IA), respectively. When IA is used, each satellite aggregates its gradient updates with the received ones, according to the method described in Section IV-A. Without IA, each satellite only forwards its gradients and the received ones to the other satellite or the PS, without performing any aggregation. We have evaluated the total transmitted data for different sparsification ratios $q = 0.01$, $q = 0.1$, as well as without sparsification, which corresponds to $q = 1$.

Fig. 6a shows the number of the transmitted elements for different sparsification ratios, normalized with the length of the sparsified gradient vector n_a . Clearly, this comparison is only meaningful if the IA does not affect the model accuracy and we have verified that this is the case since when IA is applied, satellites only perform the aggregation operations, which is equivalent to the operations performed by the PS without IA. The final parameter values obtained, with or without IA, remain unchanged. By comparing the cases with and without IA, we can observe a significant reduction in the transmission load when the number of satellites increases, > 10 times with 40 satellites and no sparsification. This reduction is particularly valuable as the number of global iterations increases since it consistently reduces the transmitted data in each iteration, thereby addressing the problem of overall communication cost in FL. In addition to the simulation curves, Fig. 6a also depicts and verifies the theoretical upper bound for the transmission load, derived in Section V.

The normalized transmitted data increases as the sparsification ratio q increases. To explain this, recall that, when IA is applied under the assumption of sparsification, the satellites transmit the non-zero elements along with their respective indices. When the indices of non-zero elements differ among satellites, each satellite must transmit its own elements and the elements from the other satellites, along with their indices. This leads to an increase in the number of elements transmitted. However, as the sparsification ratio q increases, it becomes more likely that the same indices will have the non-zero entries at different satellites. Each index that is present at multiple satellites needs to be transmitted only once, along with the aggregated value from all the satellites, which reduces the transmitted data.

Fig. 6b shows the absolute value, rather than the normalized, of the total transmitted data. The storage size of each element ω is set to 32 bits. For the case with IA, with sparsification ($q > 1$), a total number of 45 bits is required to transmit each element, which is the sum of the storage

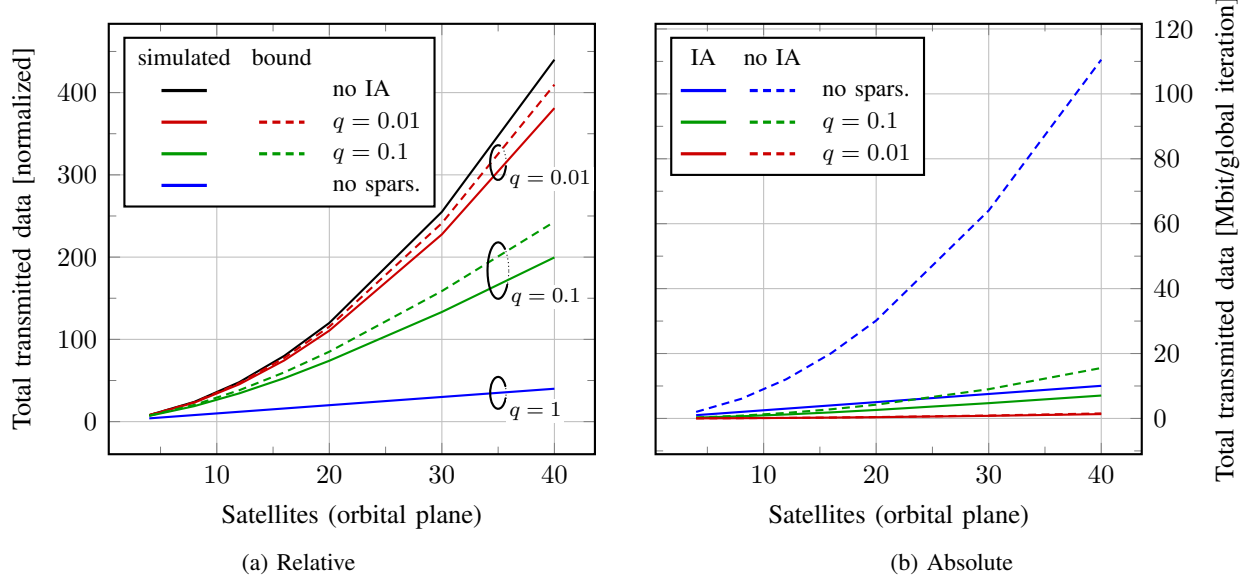


Fig. 6. Total transmission data in one global iteration for three different sparsification ratios; a) $q = 0.01$ and b) $q = 0.1$, and c) without sparsification ($q=1$). IA and no IA stand for the proposed algorithm with and without incremental aggregation respectively.

space for each element and its index. In the considered model, the index storage space is 13 bits. The difference between the schemes with and without IA becomes substantial as q increases, owing to the increased correlation among the indices of non-zero elements across the satellites. Additionally, when the number of satellites increases, the reduction in data size achieved with IA is significant to the extent that the case without sparsification $q = 1$ outperforms the case without IA and a sparsification ratio of $q = 0.1$.

The proposed FedAvg with ISL effectively offloads communication from GSLs to ISLs. This is especially relevant due to the fact that the ISLs are increasingly implemented as high-throughput optical links [59]. When FedAvg with ISL is used, the number of required GSLs is independent of the number of satellites in each orbit and remains constant at 2 for each global iteration, one for uplink and one for downlink, respectively. However, when FedAvg does not use ISLs, the number of GSLs increases linearly with the number of satellites, as each satellite has to transmit and receive the parameters on its own.

VII. DISCUSSION AND CONCLUSIONS

We have designed a clustered FL system tailored to distributed ML in modern satellite mega-constellations. It efficiently uses ISLs to avoid connectivity bottlenecks that impair convergence

speed. Owing to a FL-specific in-network aggregation strategy, this is achieved without increasing the total transmitted amount of data. Indeed, it can be expected that this method actually decreases the communication cost due to relying on cheaper-to-operate ISLs instead of long distance GSLs. Moreover, the communication load is evenly spread among the network instead of focusing all communications on direct worker-to-PS links. This strategy requires a careful predictive route planning in order to operate successfully in a dynamic network topology imposed by orbital mechanics. We have developed the necessary routing algorithms for this in conjunction with a rigorous distributed system design that inflicts a low overhead for synchronization and consensus finding. The proposed system is compatible with a wide variety of FL algorithms, supports gradient sparsification, and includes facilities for asynchronous clustered aggregation. While not explicitly mentioned, the system's extension to incorporate worker scheduling is rather straightforward. We have evaluated the performance of the proposed system for a few carefully chosen examples. The results highlight the major increase in convergence speed to to ISLs and the bandwidth effectiveness of our in-network aggregation approach.

Regarding future work, it is interesting to revise the assumption adopted in this paper that all participants in the FL process are trustworthy, under complete control, and the software operates nominally. For instance, if the satellites belong to different operators, the use of ISLs may incur a certain cost and/or a group of satellites may decide not to participate in the FL process, which would require an extension of the proposed algorithms.

REFERENCES

- [1] N. Razmi, B. Matthiesen, A. Dekorsy, and P. Popovski, “On-board federated learning for dense LEO constellations,” in *IEEE Int. Conf. Commun. (ICC)*, Seoul, Korea, May 2022.
- [2] M. Sweeting, “Modern small satellites - changing the economics of space,” *Proc. IEEE*, vol. 106, no. 3, pp. 343–361, 2018.
- [3] I. Leyva-Mayorga *et al.*, “LEO small-satellite constellations for 5G and beyond-5G communications,” *IEEE Access*, vol. 8, pp. 184 955–184 964, 2020.
- [4] M. Y. Abdelsadek *et al.*, “Future space networks: Toward the next giant leap for humankind,” *IEEE Trans. Commun.*, vol. 71, no. 2, pp. 949–1007, Feb. 2023.
- [5] M. Mozaffari, X. Lin, and S. Hayes, “Toward 6g with connected sky: Uavs and beyond,” *IEEE Commun. Mag.*, vol. 59, no. 12, pp. 74–80, 2021.
- [6] H. Chen, M. Xiao, and Z. Pang, “Satellite-based computing networks with federated learning,” *IEEE Wireless Commun.*, vol. 29, no. 1, pp. 78–84, Feb. 2022.
- [7] B. Matthiesen, N. Razmi, I. Leyva-Mayorga, A. Dekorsy, and P. Popovski, “Federated learning in satellite constellations,” *IEEE Netw.*, 2023, early access.
- [8] D. Izzo *et al.*, “Selected trends in artificial intelligence for space applications,” Dec. 2022.

- [9] G. Fontanesi *et al.*, “Artificial intelligence for satellite communication and non-terrestrial networks: A survey,” Apr. 2023.
- [10] N. Razmi, B. Matthiesen, A. Dekorsy, and P. Popovski, “Ground-assisted federated learning in LEO satellite constellations,” *IEEE Wireless Commun. Lett.*, vol. 11, no. 4, pp. 717–721, 2022.
- [11] R. Radhakrishnan *et al.*, “Survey of inter-satellite communication for small satellite systems: Physical layer to network layer view,” *IEEE Commun. Surveys Tuts.*, vol. 18, no. 4, pp. 2442–2473, 2016.
- [12] Y. Lee and J. P. Choi, “Connectivity analysis of mega-constellation satellite networks with optical intersatellite links,” *IEEE Trans. Aerosp. Electron. Syst.*, vol. 57, no. 6, pp. 4213–4226, 2021.
- [13] R. Li, B. Lin, Y. Liu, M. Dong, and S. Zhao, “A survey on laser space network: Terminals, links, and architectures,” *IEEE Access*, vol. 10, pp. 34 815–34 834, 2022.
- [14] E. Fasolo, M. Rossi, J. Widmer, and M. Zorzi, “In-network aggregation techniques for wireless sensor networks: a survey,” *IEEE Wireless Commun.*, vol. 14, no. 2, pp. 70–87, 2007.
- [15] J. Wang *et al.*, “A field guide to federated optimization,” Jul. 2021. [Online]. Available: <https://arxiv.org/abs/2107.06917>
- [16] Q.-V. Pham, M. Zeng, T. Huynh-The, Z. Han, and W.-J. Hwang, “Aerial access networks for federated learning: Applications and challenges,” *IEEE Netw.*, vol. 36, no. 3, pp. 159–166, May 2022.
- [17] Q. Fang *et al.*, “Olive branch learning: A topology-aware federated learning framework for space-air-ground integrated network,” *IEEE Trans. Wireless Commun.*, 2022, early access.
- [18] R. Uddin and S. Kumar, “SDN-based federated learning approach for satellite-IoT framework to enhance data security and privacy in space communication,” in *IEEE Int. Conf. Wireless Space Extreme Environ. (WiSEE)*, MB, Canada, Oct. 2022.
- [19] N. Razmi, B. Matthiesen, A. Dekorsy, and P. Popovski, “Scheduling for ground-assisted federated learning in LEO satellite constellations,” in *Eur. Signal Process. Conf. (EUSIPCO)*, Belgrade, Serbia, Aug. 2022.
- [20] J. So *et al.*, “FedSpace: An efficient federated learning framework at satellites and ground stations,” Feb. 2022.
- [21] L. Wu and J. Zhang, “FedGSM: Efficient federated learning for LEO constellations with gradient staleness mitigation,” Apr. 2023. [Online]. Available: <https://arxiv.org/abs/2304.08537>
- [22] J. Lin, J. Xu, Y. Li, and Z. Xu, “Federated learning with dynamic aggregation based on connection density at satellites and ground stations,” in *IEEE Int. Conf. Satell. Comput. (Satellite)*, Shenzhen, China, Nov. 2022.
- [23] M. Elmahallawy and T. Luo, “FedHAP: Fast federated learning for LEO constellations using collaborative HAPs,” Sep. 2022. [Online]. Available: <https://arxiv.org/abs/2205.07216>
- [24] ——, “AsyncFLEO: Asynchronous federated learning for LEO satellite constellations with high-altitude platforms,” in *IEEE Int. Conf. Big Data*, Osaka, Japan, Dec. 2022.
- [25] ——, “Optimizing federated learning in LEO satellite constellations via intra-plane model propagation and sink satellite scheduling,” Feb. 2023. [Online]. Available: <https://arxiv.org/abs/2302.13447>
- [26] C.-Y. Chen, L.-H. Shen, K.-T. Feng, L.-L. Yang, and J.-M. Wu, “Edge selection and clustering for federated learning in optical inter-LEO satellite constellation,” Apr. 2023. [Online]. Available: <https://arxiv.org/abs/2303.16071>
- [27] C. Wu, Y. Zhu, and F. Wang, “DSFL: Decentralized satellite federated learning for energy-aware LEO constellation computing,” in *IEEE Int. Conf. Satell. Comput. (Satellite)*, Shenzhen, China, Nov. 2022.
- [28] J. Östman, P. Gomez, V. M. Shreenath, and G. Meoni, “Decentralised semi-supervised onboard learning for scene classification in low-earth orbit,” May 2023. [Online]. Available: <https://arxiv.org/abs/2305.04059>
- [29] P. Wang, H. Li, and B. Chen, “FL-task-aware routing and resource reservation over satellite networks,” in *IEEE Global Commun. Conf. (GLOBECOM)*, Rio de Janeiro, Brazil, Dec. 2022.
- [30] 3GPP, “Study on New Radio (NR) to support non-terrestrial networks,” Tech. Rep. TR 38.811 V15.4.0, Sep. 2020.
- [31] D. Bhattacherjee and A. Singla, “Network topology design at 27,000 km/hour,” in *Int. Conf. Emerg. Netw. Exp. Technol.*, FL, USA, Dec. 2019.

- [32] I. Leyva-Mayorga, B. Soret, and P. Popovski, “Inter-plane inter-satellite connectivity in dense LEO constellations,” *IEEE Trans. Wireless Commun.*, vol. 20, no. 6, pp. 3430–3443, 2021.
- [33] B. McMahan, E. Moore, D. Ramage, S. Hampson, and B. Agüera y Arcas, “Communication-efficient learning of deep networks from decentralized data,” in *Artif. Intell. Statist. (AISTATS)*, FL, USA, Apr. 2017.
- [34] A. P. Miettinen and J. K. Nurminen, “Energy efficiency of mobile clients in cloud computing,” in *USENIX Workshop Hot Top. Cloud Comput.*, Boston, USA, Jun. 2010.
- [35] K. Scott and S. C. Burleigh, “Bundle protocol specification,” RFC 5050, Tech. Rep. 5050, Nov. 2007.
- [36] S. Burleigh, K. Fall, and E. J. Birrane, “Bundle protocol version 7,” RFC 9171, Tech. Rep. 9171, Jan. 2022.
- [37] D. P. Bertsekas and J. N. Tsitsiklis, *Parallel and Distributed Computation: Numerical Methods*. Athena Scientific, 2015.
- [38] L. Torgerson *et al.*, “Delay-tolerant networking architecture,” RFC 4838, Tech. Rep. 4838, Apr. 2007.
- [39] G. Araniti *et al.*, “Contact graph routing in DTN space networks: overview, enhancements and performance,” *IEEE Commun. Mag.*, vol. 53, no. 3, pp. 38–46, 2015.
- [40] J. A. Fraire, O. D. Jonckère, and S. C. Burleigh, “Routing in the space internet: A contact graph routing tutorial,” *J. Netw. Comput. Appl.*, vol. 174, 2021.
- [41] N. Deo, *Graph theory with applications to engineering and computer science*. Prentice-Hall, 1974.
- [42] J. R. Vetter, “Fifty years of orbit determination: Development of modern astrodynamics methods,” *Johns Hopkins APL Technical Digest*, vol. 27, no. 3, pp. 239–252, 2007.
- [43] D. Vallado and P. Crawford, “SGP4 orbit determination,” in *Astrodyn. Spec. Conf. Exhib.*, Aug. 2008.
- [44] D. A. Vallado and W. D. McClain, *Fundamentals of Astrodynamics and Applications*, 4th ed. Microcosm Press, 2013.
- [45] D. A. Vallado, P. Crawford, R. Hujasak, and T. S. Kelso, “Revisiting spacetrack report #3: Rev 3,” AIAA, Tech. Rep., 2007.
- [46] F. R. Hoots and R. L. Roehrich, “Models for propagation of NORAD element sets,” Project Space Track, Aerospace Defense Command, Tech. Rep. Spacetrack Report No. 3, Dec. 1980.
- [47] A. F. Aji and K. Heafield, “Sparse communication for distributed gradient descent,” in *Empir. Methods Nat. Lang. Process.*, Copenhagen, Denmark, Sep. 2017.
- [48] D. Alistarh *et al.*, “The convergence of sparsified gradient methods,” in *NeurIPS*, Dec. 2018.
- [49] I. S. Duff, A. M. Erisman, and J. K. Reid, *Direct Methods for Sparse Matrices*, 2nd ed. Oxford Univ. Press, Jan. 2017.
- [50] A. W. van der Vaart, *Asymptotic Statistics*. Cambridge, U.K.: Cambridge Univ. Press, 1998.
- [51] I. Leyva-Mayorga *et al.*, “NGSO constellation design for global connectivity,” in *Non-Geostationary Satellite Communications Systems*, E. Lagunas, S. Chatzinotas, K. An, and B. F. Beidas, Eds. Hertfordshire, UK: IET, Dec. 2022, ch. 9, pp. 189–236.
- [52] L. J. Ippolito Jr, *Satellite Communications Systems Engineering*. John Wiley & Sons, 2017.
- [53] Y. LeCun, C. Cortes, and C. J. C. Burges. The MNIST database of handwritten digits. [Online]. Available: <http://yann.lecun.com/exdb/mnist/>
- [54] Y. Fraboni, R. Vidal, L. Kameni, and M. Lorenzi, “A general theory for federated optimization with asynchronous and heterogeneous clients updates,” *J. of Mach. Learn. Res.*, vol. 24, no. 110, pp. 1–43, 2023.
- [55] A. Krizhevsky and G. Hinton, “Learning multiple layers of features from tiny images,” University of Toronto, MSc Thesis, Apr. 2009. [Online]. Available: <https://www.cs.toronto.edu/~kriz/cifar.html>
- [56] M. Yurochkin *et al.*, “Bayesian nonparametric federated learning of neural networks,” in *ICML*, California, USA, Jun. 2019.
- [57] H. Wang, M. Yurochkin, Y. Sun, D. Papailiopoulos, and Y. Khazaeni, “Federated learning with matched averaging,” in *Int. Conf. Learn. Repr. (ICLR)*, Apr. 2020.
- [58] C. He *et al.*, “FedML: A research library and benchmark for federated machine learning,” in *NeurIPS*, Dec. 2020.
- [59] Z. Sodnik, B. Furch, and H. Lutz, “Optical intersatellite communication,” *IEEE J. Sel. Topics Quantum Electron.*, 2010.